HTML ABSTRACT + LINKS

Dispersion relations for the convective instability of an acidity front in Hele-Shaw cells

Desiderio A. Vasquez
Department of Physics, Indiana University Purdue, University Fort Wayne, Fort Wayne, Indiana 46805

A. De Wit
Service de Chimie Physique and Centre for Nonlinear Phenomena and Complex Systems, Case Postale 231, Université Libre de Bruxelles, 1050 Brussels, Belgium

(Received 3 February 2004; accepted 19 April 2004)

Autocatalytic chemical fronts of the chlorite-tetrathionate (CT) reaction become buoyantly unstable when they travel downwards in the gravity field because they imply an unfavorable density stratification of heavier products on top of lighter reactants. When such a density fingering instability occurs in extended Hele-Shaw cells, several fingers appear at onset which can be characterized by dispersion relations giving the growth rate of the perturbations as a function of their wave number. We analyze here theoretically such dispersion curves comparing the results for various models obtained by coupling Darcy's law or Brinkman's equation to either a one-variable reaction-diffusion model for the CT reaction or an eikonal equation. Our theoretical results are compared to recent experimental data. © *2004 American Institute of Physics.*
[DOI: 10.1063/1.1760515]

I. INTRODUCTION

Chemical autocatalytic propagating fronts can become hydrodynamically buoyantly unstable if they feature a density change across the front such that the heavier solution lies on top of the lighter one in the gravity field.[1] Recent experiments have analyzed such an instability in Hele-Shaw cells,[2–9] two planar glass plates of large lateral extent separated by a thin gap width. In such a geometry, the convective instability of the front induced by the unfavorable density stratification leads to a fingering of the front characterized by several wavelengths. In contrast to similar experiments performed in capillary tubes for which only one or two convection rolls can develop,[10–12] experimental results in extended Hele-Shaw cells allow us to have insight into dispersion relations featuring the growth rate σ of the perturbations as a function of their wave number k. Such dispersion relations have been measured experimentally for the iodate-arsenious acid (IAA) reaction[4,5] as well as for the chlorite-tetrathionate (CT) reaction.[6–9] They show that a band of unstable modes exists ranging typically from $k=0$ to a critical value k_c. Recently, Horváth *et al.* have analyzed experimentally the influence of a tilt of the Hele-Shaw cell with regard to the vertical on the dispersion relation for the CT reaction.[6] They compare their results with theoretical predictions for isothermal reactions based either on Darcy's law coupled to a reaction-diffusion model of the CT reaction,[13] to Navier-Stokes equation coupled to a thin front approximation for the chemical system,[14,15] and to a model involving surface tension effects. While the latter description does not seem to be appropriate, no definitive conclusion could be drawn between the two former theoretical models. In addition, Bánsági *et al.* have also analyzed the instability in Hele-Shaw cells of variable thickness[7] showing that the convectively unstable regime increases as the gap width increases. From the dispersion curves, they have then determined quantitatively the influence of the gap width change on the characteristics of the most unstable mode. Further experiments demonstrate that, as the CT reaction is exothermic, an increase of the gap also leads to more pronounced heat effects.[7,8] On the basis of Darcy's law coupled to an evolution equation for both the concentration and the temperature, it has been shown theoretically that heat effects can qualitatively change the characteristics of the dispersion curves.[8,16] This enlightens the fact that, even in very thin Hele-Shaw cells for which Darcy's law is valid, the coupling between solutal and thermal effects can affect the nature of dispersion curves. In this context, it is necessary to check the influence of the hydrodynamic description of the fluid velocity on the dispersion curves. Martin *et al.*[5,17] as well as Demuth and Meiburg[18] have shown on the IAA reaction that two-dimensional (2D) Brinkman and 3D Stokes models do a better job in capturing quantitatively dispersion curves for thicker Hele-Shaw cells although no qualitative change with regard to a 2D Darcy description is introduced. It is our objective here to perform a similar analysis for the CT system and compare various descriptions of the system (Darcy or Brinkman's equations coupled either to the full reaction-diffusion model or to a simple eikonal equation) to experimental dispersion curves. Although heat effects should be more pronounced when the gap width increases, we explicitely do not consider here an evolution equation for the temperature. Instead we compare dispersion curves for a total density jump across the front, respectively, with or without the thermal contribution. This allows us to focus essentially on the quantitative changes related to 2D versus 3D description of the flow rather than on the competition between heat

 © 2004 American Institute of Physics

Downloaded 09 Jul 2004 to 128.111.72.135. Redistribution subject to AIP license or copyright, see http://jcp.aip.org/jcp/copyright.jsp

and solutal effects. In this perspective, we introduce the various models in Sec. I A and then discuss the results in Sec. II B.

A. Equations of motion

Our system is a Hele-Shaw cell of width L_x, length L_z, and gap width a in which an acid catalyzed CT chemical front travels along the z direction pointing upwards along the gravity field. The transverse coordinate is x. To model the chemical reactions, we use two different points of view, i.e., the full reaction-diffusion system or the eikonal relation. Assuming that all chemical species diffuse with the same diffusion coefficient D, the reaction-diffusion-advection model for the isothermal CT reaction is[8,13,16]

$$\frac{\partial \alpha}{\partial t}+\vec{V}\cdot\vec{\nabla}\alpha=D\nabla^2\alpha-36\gamma\alpha_0^3\alpha(1-\alpha)^2(\kappa+7\alpha), \quad (1)$$

where α is the concentration of tetrathionate ions nondimensionalized by α_0, its value at initial time, γ is the kinetic constant, and where $\kappa=2[\mathrm{ClO}_2^-]_0/\alpha_0-7$ (fixed to $\kappa=1$ here). $\vec{V}$ is the two-dimensional fluid velocity.

The front propagation is also alternatively modeled using an eikonal relation

$$c=c_0+DK+\vec{V}\cdot\hat{n}, \quad (2)$$

which relates the normal speed of the front c to the flat front speed c_0, the curvature of the front K, and the coefficient of molecular diffusivity D. Here, $\hat{n}$ is the unit vector in the direction normal to the front, pointing towards the unreacted fluid. In Hele-Shaw cells, the evolution equation for the gap-averaged 2D flow velocity $\vec{V}$ is given by

$$\frac{\partial \vec{V}}{\partial t}+\frac{6}{5}(\vec{V}\cdot\vec{\nabla})\vec{V}=-\frac{1}{\rho_0}\vec{\nabla}p+\nu\nabla^2\vec{V}-12\frac{\nu}{a^2}\vec{V}-\frac{\rho}{\rho_0}g\hat{z}, \quad (3)$$

where $\rho=\rho(\alpha)$ is the density of the solution and ρ_0 that of pure water, a is the gap width between the two cells, and ν is the kinematic viscosity. The pressure p can be eliminated using the vorticity ω-stream function ψ formulation,

$$\frac{\partial \omega}{\partial t}=\nu\nabla^2\omega-12\frac{\nu}{a^2}\omega+g\frac{\partial \Delta\rho}{\partial x}+\frac{6}{5}\frac{\partial(\psi,\omega)}{\partial(x,z)}, \quad (4)$$

with $\nabla^2\psi=\omega$ and $\partial(\psi,\omega)/\partial(x,z)=\psi_x\omega_z-\psi_z\omega_x$, where the subscript denotes partial derivative. Here, $\Delta\rho$ is the fractional density difference between the densities of the reacted ρ_r and unreacted ρ_u solutions, i.e., $\Delta\rho=(\rho_r-\rho_u)/\rho_r$. Let us recall that, for the CT reaction, $\rho_r>\rho_u$, hence $\Delta\rho>0$. Using $\tau=1/36\gamma\alpha_o^3$ as a chemical unit of time, defining $L=(D\tau)^{1/2}$ as unit of length, and assuming a linear dependence between density and the concentration, we rewrite the coupled system of equations in dimensionless variables:

$$\frac{\partial \alpha}{\partial t}=\frac{\partial(\psi,\alpha)}{\partial(x,z)}+\nabla^2\alpha-\alpha(1-\alpha)^2(\kappa+7\alpha), \quad (5)$$

$$\frac{\partial \omega}{\partial t}=S_c\nabla^2\omega-S_c\frac{12L^2}{a^2}\omega-S_c\mathrm{Ra}\frac{\partial \alpha}{\partial x}+\frac{6}{5}\frac{\partial(\psi,\omega)}{\partial(x,z)}. \quad (6)$$

The parameter $S_c=\nu/D$ is the Schmidt number and $\mathrm{Ra}=g\Delta\rho L^3/\nu D$ is the Rayleigh number. We solve all our calculations in the limit of infinite Schmidt number, which corresponds to the experimental situation.[8] In that case, Eq. (6) yields Brinkman's equation,

$$\nabla^2\omega-\frac{12L^2}{a^2}\omega-\mathrm{Ra}\frac{\partial \alpha}{\partial x}=0. \quad (7)$$

In the limit $a\to 0$, Brinkman's equation reduces to Darcy's law,

$$\omega=\nabla^2\psi=-\frac{a^2}{12L^2}\mathrm{Ra}\frac{\partial \alpha}{\partial x}=-\mathrm{Ra}_p\frac{\partial \alpha}{\partial x}, \quad (8)$$

where we have introduced the Rayleigh number for porous media $\mathrm{Ra}_p=g\Delta\rho La^2/12\nu D=\mathrm{Ra}\ a^2/12L^2$. For $a\to\infty$, Brinkman's equation recovers the unbounded geometry case (thick cells).

Let us now analyze the stability of the front solution comparing various models. We will consider successively Brinkman's equation (7) or Darcy's law (8) coupled to the reaction-diffusion-advection equation (5) which we will refer to as BRD and DRD models, respectively. These flow equations can also be coupled to the eikonal equation (2) to yield the Brinkman-eikonal (BE) or Darcy-eikonal (DE) model.

B. Numerical solutions

We calculate the dispersion relations by linearizing the reaction-diffusion-convection equations around the convectionless flat front solution as carried out for the IAA reaction in Refs. 5, 17–20 and for the CT reaction in Refs. 8, 13, 16. The variables are expanded as $\alpha=\alpha^{(0)}+\alpha^{(1)}$, $\psi=\psi^{(1)}$, where the zero-order solution corresponds to the convectionless traveling front solution. However, in the present case, an analytic solution for the convectionless front is not available. This base state solution is found numerically by a finite-difference integration of Eq. (4) with no fluid motion to obtain the basic convectionless solution.[13] Once the equations are linearized, we introduce wavelike perturbations of the form

$$\alpha^{(1)}=\alpha(z)e^{\sigma t}e^{ikx} \quad (9)$$

and

$$\psi^{(1)}=\psi(z)e^{\sigma t}e^{ikx}, \quad (10)$$

which leads to an eigenvalue equation for σ parametrized by the wave number k. The eigenvalue system of linear equations is solved using a modified power method.[21]

In the case of the eikonal relation, the fluid motion is still described by Darcy's law and Brinkman's equations. The reaction front is treated by a time-dependent front height $z=h(x,t)$. This allows us to approximate the front curvature $K\simeq\partial^2h/\partial x^2$. Therefore the linearized eikonal relation is written as

$$\frac{\partial h}{\partial t}-V_z|_{z=h}=c_0+D\frac{\partial^2 h}{\partial x^2}. \quad (11)$$

The change in density across the front leads to jump conditions in the stream function and its derivates.[23]

Downloaded 09 Jul 2004 to 128.111.72.135. Redistribution subject to AIP license or copyright, see http://jcp.aip.org/jcp/copyright.jsp

II. RESULTS

Our dispersion relations are computed in dimensionless variables to provide dimensionless dispersion curves $\sigma = \sigma(k)$. In order to make quantitative comparisons with experimental dispersion curves, we must have an estimate of the characteristic time $\tau = 1/36\gamma\alpha_o^3$ and length $L = (D\tau)^{1/2}$. There is currently discrepancies in the literature on the value of the kinetic constant γ which impairs the possible comparisons between theoretical and experimental results.[13] Facing this difficulty, we have nevertheless chosen to attempt such a comparison by using the value of γ computed in Yang *et al.* in previous modeling of fingering in the CT reaction.[13] For a one-variable kinetic model of the CT reaction, i.e., assuming that the tetrathionate α and proton β species have the same diffusion coefficient (i.e., $\delta = D_\alpha/D_\beta = 1$), Yang *et al.*'s equations suggest that $\gamma = c_o^2/100D\alpha_o^3$. This value of γ matches the experimental convectionless front speed. We take here $D = 1.2\times10^{-2}$ mm^2/s, which is the diffusion coefficient of protons, the autocatalytic species that set up the speed of the front. For $\alpha_o = 5\times10^{-3}$ M and a planar front of speed $c_o = 0.12$ mm/s, we get then $\gamma = 9.6\times10^4$ M^3 s^{-1}. Hence we find that $\tau = 2.24$ s while $L = 0.1641$ mm. With these values, we can compute the Rayleigh number $\mathrm{Ra} = gL^3\Delta\rho/\nu D$ appearing in Brinkman's equation (7) for a given density difference $\Delta\rho$. As an example, for $g = 9.8\times10^3$ mm/s, $\nu = 0.99$ mm^2/s, and the above values of L and D, we find $\mathrm{Ra} = 1.38$ for $\Delta\rho = 3.8\times10^{-4}$, for instance, or also $\mathrm{Ra} = 1.13$ for $\Delta\rho = 3.1\times10^{-4}$. For a given gap width a, we can then also compute the Rayleigh number for porous media appearing in Darcy's law (8) as $\mathrm{Ra}_p = gLa^2\Delta\rho/12\nu D$.

In the experiments conducted by Horváth *et al.* and focusing on 2D versus 3D effects,[6,7] the chemical composition is kept to $\alpha_o = 5\times10^{-3}$ M while $D = 1.2\times10^{-2}$ mm^2 s^{-1}. As the CT reaction is exothermic, heat release can contribute to the density change.[7,8,16] The total density variation across the front is therefore the sum of a solutal $\Delta\rho_S$ and thermal $\Delta\rho_T$ contribution, i.e., $\Delta\rho = \Delta\rho_S + \Delta\rho_T$. The isothermal $\Delta\rho_S$ does not depend on the gap width but varies with chemical composition.[9] For the CT reaction, $\Delta\rho_S$ is equal to 3.8×10^{-4} for $\alpha_o = 5\times10^{-3}$ M.[6,7] The thermal density jump on the contrary highly depends on the gap width. For $a\to0$, all the heat produced by the reaction is rapidly dissipated through the walls and $\Delta\rho_T\sim0$. When a is increased, heat effects become important. In the present work, we do not include explicitly the heat equation, therefore we analyze the limiting cases of zero, infinite, and intermediate thermal diffusivity. For zero thermal diffusivity, the reacted and unreacted fluids are set at their final temperatures. In that case, the thermal contribution to the density jump has been measured to be equal to $\Delta\rho_T = -1.2\times10^{-4}$ giving a net density change $\Delta\rho = 2.6\times10^{-4}$.[7] In the case of infinite thermal diffusivity, both fluids are at the higher temperature of the reacted fluid. Consequently, we need to consider the value of the change due to solutal concentrations only and $\Delta\rho = 3.8\times10^{-4}$ (since both fluids are at the same higher temperature). To analyze the intermediate regime, we choose in addition an intermediate value of $\Delta\rho = 3.1\times10^{-4}$. Detailed calculations have shown that in the IAA reaction the transition to convection in capillary tubes is well approximated by the limit of infinite thermal diffusivity.[22]

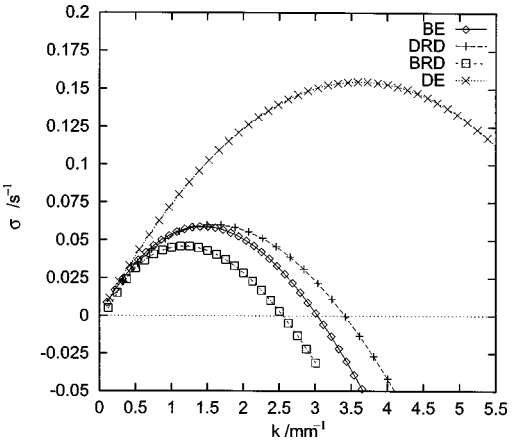

FIG. 1. Dimensional dispersion relation for a cell of width $a = 0.821$ mm and $\Delta\rho = 3.1\times10^{-4}$ ($\mathrm{Ra} = 1.13$, $\mathrm{Ra}_p = 2.36$). Four different models are compared: Darcy and eikonal (DE), Darcy and reaction-diffusion (DRD), Brinkman and eikonal (BE), and Brinkman and reaction-diffusion (BRD).

The parameters that are varied experimentally are the gap width a (Ref. 7) and the angle θ between the plates and the vertical[6] which modifies the Rayleigh number according to $\mathrm{Ra}\sim g\cos(\theta)$. Let us now compare for some given values of experimental parameters, dispersion curves computed theoretically using the various BRD, DRD, BE, and DE models. This analysis will show that the Brinkman model provides a better description of experimental data for larger gap widths. Fixing then $a = 1.04$ mm, we will look at the effect of varying the angle θ for various density differences.

A. Dispersion relations

In this section, we compare the dispersion relations using Darcy or Brinkman descriptions for the flow coupled to, respectively, the eikonal equation or the full reaction-diffusion model. We will compare the results with experiments, therefore our dispersion curves will first be displayed in dimensional units. To compare the different models with the experimental results, we choose the value of $\Delta\rho = 3.1\times10^{-4}$, which is an intermediate value between the limits of zero and infinite thermal diffusivities.

These results are summarized in Figs. 1 and 2 featuring dispersion relations for a gap width a, respectively, equal to 0.821 mm and 1.04 mm as analyzed in Refs. 6, 7, 13. Figure 1 shows that the results obtained for $a = 0.821$ mm when coupling Darcy's law with the DE are very much different from the results obtained using the other three possible combinations. We also note that Darcy with reaction diffusion (DRD) gives a result higher than Brinkman with eikonal. The result for Brinkman with RD (BRD) is the lowest of them all. In Fig. 2, we carried out the same calculation for a larger gap of 1.04 mm. Here we do not plot the result for DE since the discrepancies with the three other ones are very large. We also note that the discrepancies between the three other descriptions are increasing in good agreement with the intuitive feeling that Darcy's law is valid in the limit $a\to0$. Similar

Downloaded 09 Jul 2004 to 128.111.72.135. Redistribution subject to AIP license or copyright, see http://jcp.aip.org/jcp/copyright.jsp

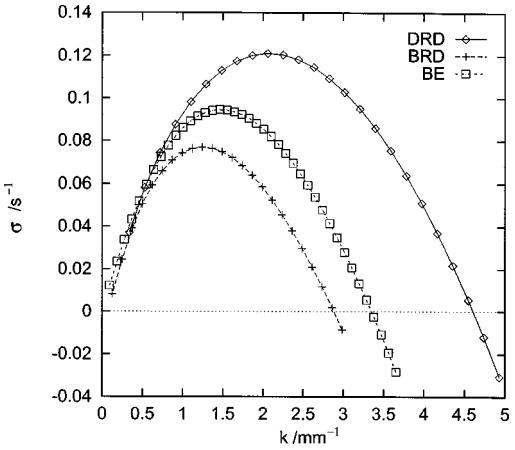

FIG. 2. Dimensional dispersion relation for a cell of width $a=1.04$ mm and $\Delta\rho=3.1\times10^{-4}$ ($\mathrm{Ra}=1.13$, $\mathrm{Ra}_p=3.78$). Three different models are compared: Darcy and reaction-diffusion (DRD), Brinkman and eikonal (BE), and Brinkman and reaction-diffusion (BRD).

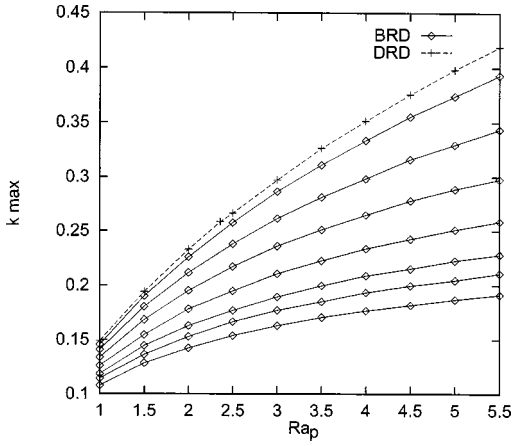

FIG. 4. The most unstable dimensionless wave number $k_{\max}$ as a function of Ra_p for different wall separations 0.2, 0.4, ..., 1.4 mm from top to bottom using both BRD and DRD models.

trends have already been discussed by Martin *et al.*[5,17] and Demuth and Meiburg[18] for the IAA reaction.

Horváth *et al.* have measured experimentally dispersion curves for the fingering of CT fronts in Hele-Shaw cells and have discussed the influence on the instability of the angle θ with vertical.[6] Let us here compare their experimental data with our theoretical curves for the three models: DRD, BE, or BRD. In Fig. 3 we compare the results of these three models computed with an angle θ such that $\cos(\theta)=0.8$. The gap separation is 1.04 mm. As we can see, the models based on Brinkman's approximation provide the best agreement to the experiments.

B. Maximum growth rate: Theory

Obviously, the Brinkman model provides the best fit to experimental data for larger gap widths. Let us now examine using nondimensional variables in which limit Darcy's law can still provide a good description.

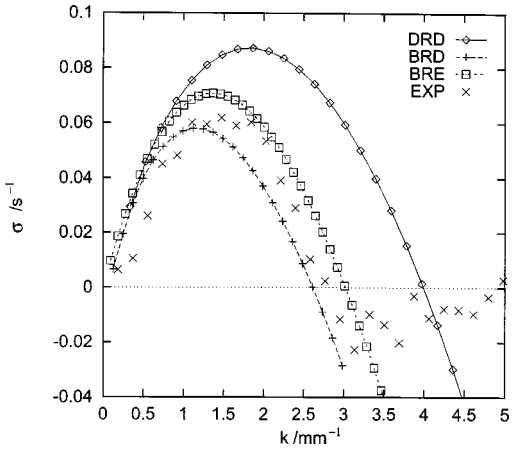

FIG. 3. Dimensional dispersion relation for a cell of width $a=1.04$ mm inclined towards the vertical with an angle θ such that $\cos(\theta)=0.8$. The experimental results (EXP) from Ref. 6 are compared with three different models computed with $\Delta\rho=3.1\times10^{-4}$: Darcy and reaction-diffusion (DRD), Brinkman and eikonal (BE), and Brinkman and reaction-diffusion (BRD).

In Figs. 4 and 5, we plot the dimensionless most unstable wave number $k_{\max}$ and the maximum growth rate $\sigma_{\max}$ as functions of the Rayleigh number for porous media (Ra_p) using Darcy and Brinkman's equations with RD. For a given fixed value of Ra_p, we can obtain various values of the couple $(\mathrm{Ra}, a/L)$. To compare both models, we solve Brinkman's equations as a function of a/L and Ra_p (instead of Ra) to analyze the small gap limit. This is accomplish by obtaining the value of Ra through the relation $\mathrm{Ra}_p=\mathrm{Ra}(a/L)^2/12$. Therefore, the figures show only one curve using Darcy's law, but several curves for Brinkman's equations. We show the variation for different wall separations, beginning with a wall separation of 0.2 mm, up to a wall separation of 1.4 mm. Quantitative conclusions are difficult to draw because varying a/L keeping Ra_p (and hence $La^2\Delta\rho$) constant can only be made by comparing situations at different $\Delta\rho$ and hence different concentrations. Nevertheless, we clearly see that Darcy's curve is closer to Brinkman's ones for the smallest a/L.

In Figs. 6 and 7, we plot the dimensionless most unstable wave number $k_{\max}$ and the maximum growth rate $\sigma_{\max}$ as

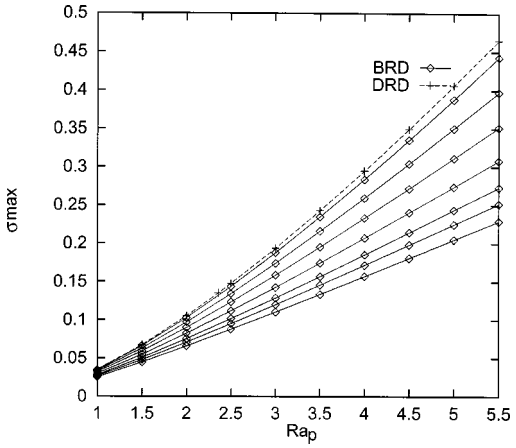

FIG. 5. The dimensionless maximum growth rate $\sigma_{\max}$ as a function of Ra_p for different wall separations 0.2, 0.4, ..., 1.4 mm from top to bottom using both BRD and DRD models.

Downloaded 09 Jul 2004 to 128.111.72.135. Redistribution subject to AIP license or copyright, see http://jcp.aip.org/jcp/copyright.jsp

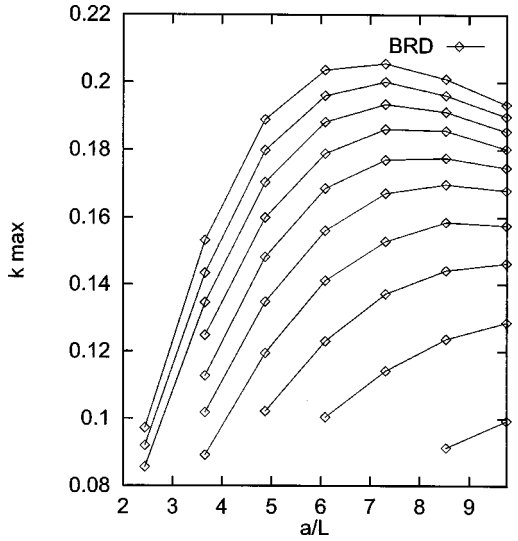

FIG. 6. The most unstable dimensionless wave number k_{max} for different values of the Rayleigh number as a function of the dimensionless gap width a/L using Brinkman's equation with RD. The top curve corresponds to Ra $=1.13$, then Ra is lowered successively by 10%.

functions of the wall separation for Brinkman with RD. We plot them for different values of the Rayleigh number Ra. In both figures, the top curve corresponds to Ra$=1.13$ and then they descend by 10% for each curve, following the equation $\mathrm{Ra}_i=1.13(0.9)^i$. That is, Ra$=1.13$, 1.07, 0.904, 0.791,.... In the experiments, Ra can easily be modified by changing the angle θ that changes g to $g\cos(\theta)$. It is interesting to note that there is a saturation for the growth rate when a is increased as observed experimentally.[7] In Fig. 8 we compare the maximum growth rate for different models as a function of gap thickness for $\Delta\rho=3.1\times10^{-4}$, i.e., Ra$=1.13$. A comparison with Fig. 5(b) of Ref. 7 shows that indeed Darcy's law seems valid up to $a=1.0-1.1$ mm but fails to account for the saturation of k_{max} correctly accounted for by Brinkman's equation. The asymptotic value of k_{max} for larger values of a (~1.75 mm^{-1} in experiments) is somewhat higher than the one predicted by Brinkman's model (~1.5 mm^{-1}).

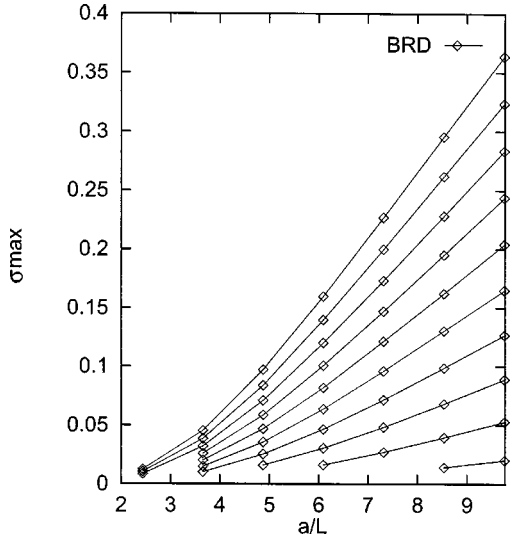

FIG. 7. The dimensionless maximum growth rate σ_{max} for different values of the Rayleigh number Ra as a function of the gap width a using Brinkman's equations with RD. The top curve corresponds to Ra$=1.13$, then Ra is lowered successively by 10%.

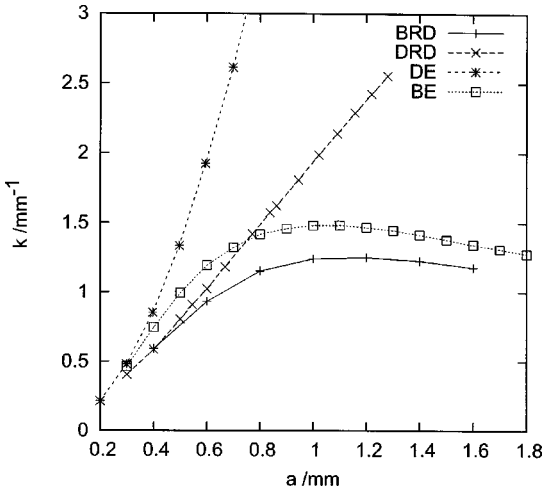

FIG. 8. The most unstable dimensionless wave number k_{max} as a function of gap width a (in mm) computed for Ra$=1.13$. Comparison is made between the four BE, BRD, DE, and DRD models. The results are close for small gaps (as expected), but they are different for larger gaps.

C. Maximum growth rate: Comparison with experiments

In Fig. 9(a) we compare the dimensional maximum growth rate σ_{max} as obtained from Horváth *et al.* experiments[6] with that from the BRD model. Similarly, we carry out the calculations for the most unstable dimensional wave number k_{max} in Fig. 9(b). The calculations were carried out for both $\Delta\rho=2.6\times10^{-4}$(Ra$=0.95$) and $\Delta\rho=3.8\times10^{-4}$(Ra$=1.38$). The exponents for $\sigma_{max}\propto\cos(\theta)^r$ are $r=1.39$ and $r=1.31$, respectively (the experimental exponent being 1.23 ± 0.18). The values for the exponent p for the curves $k_{max}\propto\cos(\theta)^p$ correspond to 0.42 and 0.37 [while, in experiments, the exponent is $p=(0.44\pm0.11)$].

Figures 10(a) and 10(b) correspond to the BE model. In this case, the exponents r for the two values of $\Delta\rho$ are, respectively, equal to 1.42 and 1.34 while the exponents p are equal to 0.39 and 0.46. The higher values of both exponents correspond to the lower value of $\Delta\rho$. It looks like both models are close to the experimental results. In all Figs. 9 and 10, the lower curve corresponds to the lower fractional density difference. With both models (eikonal and reaction-diffusion) it looks like we are close to the experiments. However, using the lower value of the density, the reaction-diffusion model falls below the experimental uncertainty, while the eikonal model is closer. This may be due to other factors that we did not take into account, for example, we assume that the tilted walls produce a convectionless state, which is not the case.

III. CONCLUSIONS

In this paper, we have compared dispersion curves for the convective instability of CT fronts in Hele-Shaw cells with experimental data available in Refs. 6 and 7. We have

Downloaded 09 Jul 2004 to 128.111.72.135. Redistribution subject to AIP license or copyright, see http://jcp.aip.org/jcp/copyright.jsp

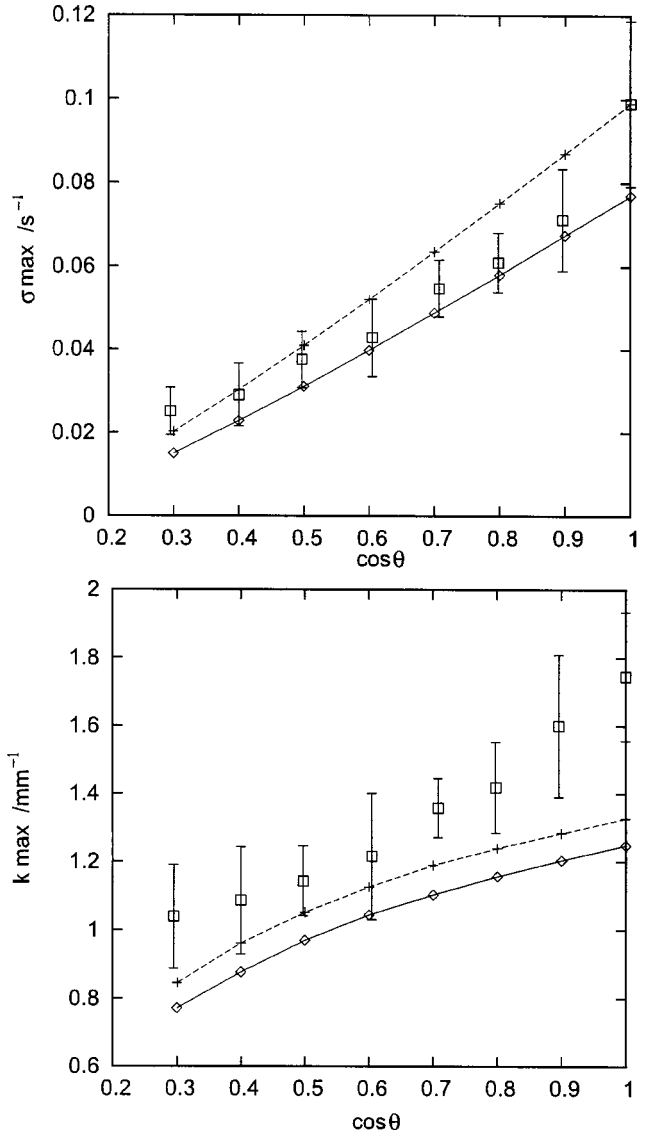

FIG. 9. The dimensional maximum growth rate (a) and most unstable wave number (b) as a function of $\cos(\theta)$. We compare the experimental results (squares with error bars) with the calculations using the BRD model and a density difference of 2.6×10^{-4} (lower solid curve) and 3.8×10^{-4} (higher broken curve). The gap is set to 1.04 mm for both cases.

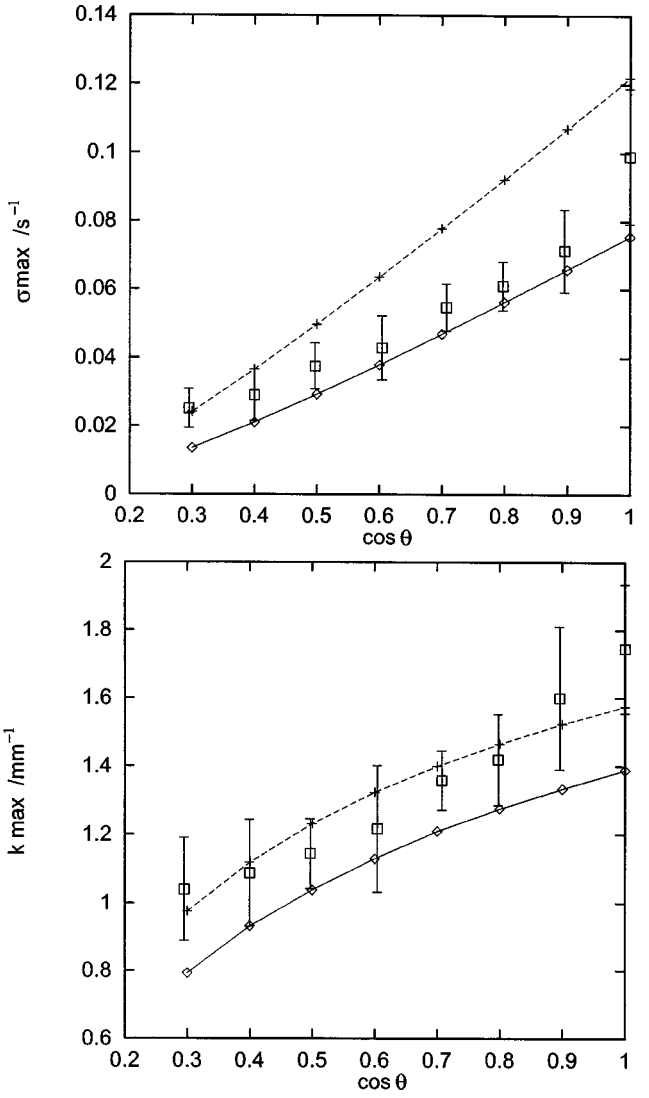

FIG. 10. The dimensional maximum growth rate (a) and most unstable wave number (b) as a function of $\cos(\theta)$. We compare the experimental results (squares with error bars) with the calculations using the BE model and a density difference of 2.6×10^{-4} (lower solid curve) and 3.8×10^{-4} (higher broken curve). The gap is set to 1.04 mm for both cases.

computed these curves using four different models resulting from coupling Darcy's law or Brinkman's equation, respectively, either to a one-variable reaction-diffusion model for the CT reaction or to an eikonal equation. While the Darcy-eikonal model is usually far off, the three other models compare favorably for small gap widths as expected. Increasing the gap width leads to poorer agreement of the Darcy-reaction-diffusion model as already discussed previously by other authors[5,17,18] without introducing any qualitative changes however. Brinkman's models provide quite good agreement with experiments. The present theoretical approach has made strong assumptions imposing that the ratio of diffusivities of the two main species $\delta=1$ and that heat effects can be incorporated using a total density jump $\Delta\rho$ incorporating the heat contribution $\Delta\rho_T$. Previous studies have shown that varying δ (Ref. 13) and taking explicitly into account the evolution equation for the temperature[8,16] can have an influence on dispersion curves so that further work to understand the influence of these effects on the 2D versus 3D description would be of interest. Our quantitative comparison with experimental data depends also on choices made on the numerical values of the kinetic constant γ and of $\Delta\rho_T$, this last parameter being strongly dependent on chemical concentrations[9] and gap width.[7] Further experimental and theoretical work are thus needed to understand in more detail the quantitative characteristics of the convective instability of chemical fronts in Hele-Shaw cells.

ACKNOWLEDGMENTS

The authors thank A. Tóth, D. Horváth, and T. Bánsági, Jr., for providing us experimental data prior to publication and for fruitful discussions. A.D. is Research Associate of the FNRS and thanks Prodex (Belgium) as well as FRFC for financial support.

Downloaded 09 Jul 2004 to 128.111.72.135. Redistribution subject to AIP license or copyright, see http://jcp.aip.org/jcp/copyright.jsp

[1] A. De Wit, Phys. Fluids **16**, 163 (2004).
[2] I. P. Nagy, A. Keresztessy, J. A. Pojman, G. Bazsa, and Z. Noszticzius, J. Phys. Chem. **98**, 6030 (1994).
[3] M. R. Carey, S. W. Morris, and P. Kolodner, Phys. Rev. E **53**, 6012 (1996).
[4] M. Böckmann and S. C. Müller, Phys. Rev. Lett. **85**, 2506 (2000).
[5] J. Martin, N. Rakotomalala, D. Salin, M. Böckmann, and S. C. Müller, J. Phys. IV **11**, 99 (2001).
[6] D. Horváth, T. Bánsági, Jr., and A. Tóth, J. Chem. Phys. **117**, 4399 (2002).
[7] T. Bánsági, Jr., D. Horváth, and A. Tóth, Phys. Rev. E **68**, 026303 (2003).
[8] T. Bánsági, Jr., D. Horváth, A. Tóth, J. Yang, S. Kalliadasis, and A. De Wit, Phys. Rev. E **68**, 05530 (R) (2003).
[9] T. Bánsági, Jr., D. Horváth, and A. Tóth, Chem. Phys. Lett. **384**, 153 (2004).
[10] I. Nagypál, G. Bazsa, and I. R. Epstein, J. Am. Chem. Soc. **108**, 3635 (1986).
[11] J. A. Pojman, I. R. Epstein, T. J. McManus, and K. Showalter, J. Phys. Chem. **95**, 1299 (1991).
[12] I. R. Epstein and J. A. Pojman, *An Introduction to Nonlinear Chemical Dynamics* (Oxford University Press, Oxford, 1998).
[13] J. Yang, A. D'Onofrio, S. Kalliadasis, and A. De Wit, J. Chem. Phys. **117**, 9395 (2002).
[14] J. Huang, D. A. Vasquez, B. F. Edwards, and P. Kolodner, Phys. Rev. E **48**, 4378 (1993).
[15] J. Huang and B. F. Edwards, Phys. Rev. E **54**, 2620 (1996).
[16] S. Kalliadasis, J. Yang, and A. De Wit, Phys. Fluids **16**, 1395 (2004).
[17] J. Martin, N. Rakotomalala, D. Salin, and M. Böckmann, Phys. Rev. E **65**, 051605 (2002).
[18] R. Demuth and E. Meiburg, Phys. Fluids **15**, 597 (2003).
[19] A. De Wit, Phys. Rev. Lett. **87**, 054502 (2001).
[20] D. A. Vasquez, B. F. Edwards, and J. W. Wilder, J. Chem. Phys. **104**, 9926 (1996).
[21] P. L. DeVries, *A First Course in Computational Physics* (Wiley, New York, 1994).
[22] D. A. Vasquez, B. F. Edwards, and J. W. Wilder, Phys. Fluids **7**, 2513 (1995).
[23] D. A. Vasquez and C. Lengacher, Phys. Rev. E **58**, 6865 (1998).

Downloaded 09 Jul 2004 to 128.111.72.135. Redistribution subject to AIP license or copyright, see http://jcp.aip.org/jcp/copyright.jsp